

Long non-coding RNA

A novel endogenous source for the generation of Dicer-like 1-dependent small RNAs in *Arabidopsis thaliana*

Xiaoxia Ma¹, Chaogang Shao², Yongfeng Jin³, Huizhong Wang^{1,*}, and Yijun Meng^{1,*}

¹College of Life and Environmental Sciences; Hangzhou Normal University; Hangzhou, P.R. China; ²College of Life Sciences; Huzhou Teachers College; Huzhou, P.R. China;

³Institute of Biochemistry; College of Life Sciences; Zhejiang University; Hangzhou, P.R. China

Keywords: lncRNA (long non-coding RNA), DCL1 (Dicer-like 1), AGO (Argonaute), degradome, dsRNA-seq (double-stranded RNA sequencing), sRNA (small RNA), *Arabidopsis thaliana*

Abbreviations: lncRNA, long non-coding RNA; sRNA, small RNA; AGO, Argonaute; pre-miRNA, precursor microRNA; pri-miRNA, primary microRNA; dsRNA-seq, double-stranded RNA sequencing; DCL1, Dicer-like 1; GEO, Gene Expression Omnibus; PLncDB, plant long non-coding RNA database; TAIR, the *Arabidopsis* information resource; RPM, reads per million; t-plot, target plot; HTS, high-throughput sequencing; *AP2*, *APETALA2*; miRNA, microRNA; Pol, polymerase; poly(A), polyadenylation; lincRNA, long intergenic non-coding RNA; PlantGSEA, the plant GeneSet enrichment analysis toolkit; rRNA, ribosomal RNA; siRNA, small interfering RNA; ARF, auxin response factor

The biological relevance of long non-coding RNAs (lncRNAs) is emerging. Whether the lncRNAs could form structured precursors for small RNAs (sRNAs) production remains elusive. Here, 172 713 DCL1 (Dicer-like 1)-dependent sRNAs were identified in *Arabidopsis*. Except for the sRNAs mapped onto the microRNA precursors, the remaining ones led us to investigate their originations. Intriguingly, 65 006 sRNAs found their loci on 5891 lncRNAs. These sRNAs were sent to AGO (Argonaute) enrichment analysis. As a result, 1264 sRNAs were enriched in AGO1, which were then subjected to target prediction. Based on degradome sequencing data, 109 transcripts were validated to be targeted by 96 sRNAs. Besides, 44 lncRNAs were targeted by 23 sRNAs. To further support the origination of the DCL1-dependent sRNAs from lncRNAs, we searched for the degradome-based cleavage signals at either ends of the sRNA loci, which were supposed to be produced during DCL1-mediated processing of the long-stem structures. As a result, 63 612 loci were supported by degradome signatures. Among these loci, 6606 reside within the dsRNA-seq (double-stranded RNA sequencing) read-covered regions of 100 nt or longer. These regions were subjected to secondary structure prediction. And, 43 regions were identified to be capable of forming highly complementary long-stem structures. We proposed that these local long-stem structures could be recognized by DCL1 for cropping, thus serving as the sRNA precursors. We hope that our study could inspire more research efforts to study on the biological roles of the lncRNAs in plants.

Introduction

With the advent of the high-throughput sequencing (HTS) technology,¹ an unexpected amount of genomic regions has been shown to be transcribed. Interestingly, a huge portion of these transcripts showed weak protein-coding capacities, which were previously called “dark matters.”^{2–4} In recent years, great efforts have been taken to uncover the biological functions of these non-coding RNAs.

MicroRNAs (miRNAs), a well-studied species of small non-coding RNAs of 20 to 24 nt in length, are critical players in diverse biological processes in eukaryotic organisms, such as cell proliferation, organ development and stress response.^{5–7} These small molecules are processed from hairpin structure-containing

precursors through two-step cropping. In plants, pri-miRNA (primary microRNA) with an internal hairpin structure is transcribed by RNA polymerase (Pol) II, resulting in poly(A) (polyadenylation) tail. The pri-miRNA is processed into pre-miRNA (precursor microRNA) through DCL1 (Dicer-like 1)-mediated cleavage. The hairpin-structured pre-miRNA is further cropped by DCL1, generating a ~21 bp-long small RNA (sRNA) duplex including miRNA and miRNA*. The mature miRNA strand is selectively incorporated into a specific AGO (Argonaute)-associated silencing complex (in most cases, the plant miRNAs are associated with the AGO1 complexes). Then, the miRNAs could guide the silencing complexes to the target transcripts based on sequence complementarity, thus enabling AGO1-mediated target cleavages.^{6,7}

*Correspondence to: Huizhong Wang; Email: whz62@163.com; and Yijun Meng; Email: mengyijun@zju.edu.cn
Submitted: 12/17/2013; Revised: 02/21/2014; Accepted: 03/31/2014; Published Online: 04/04/2014
<http://dx.doi.org/10.4161/rna.28725>

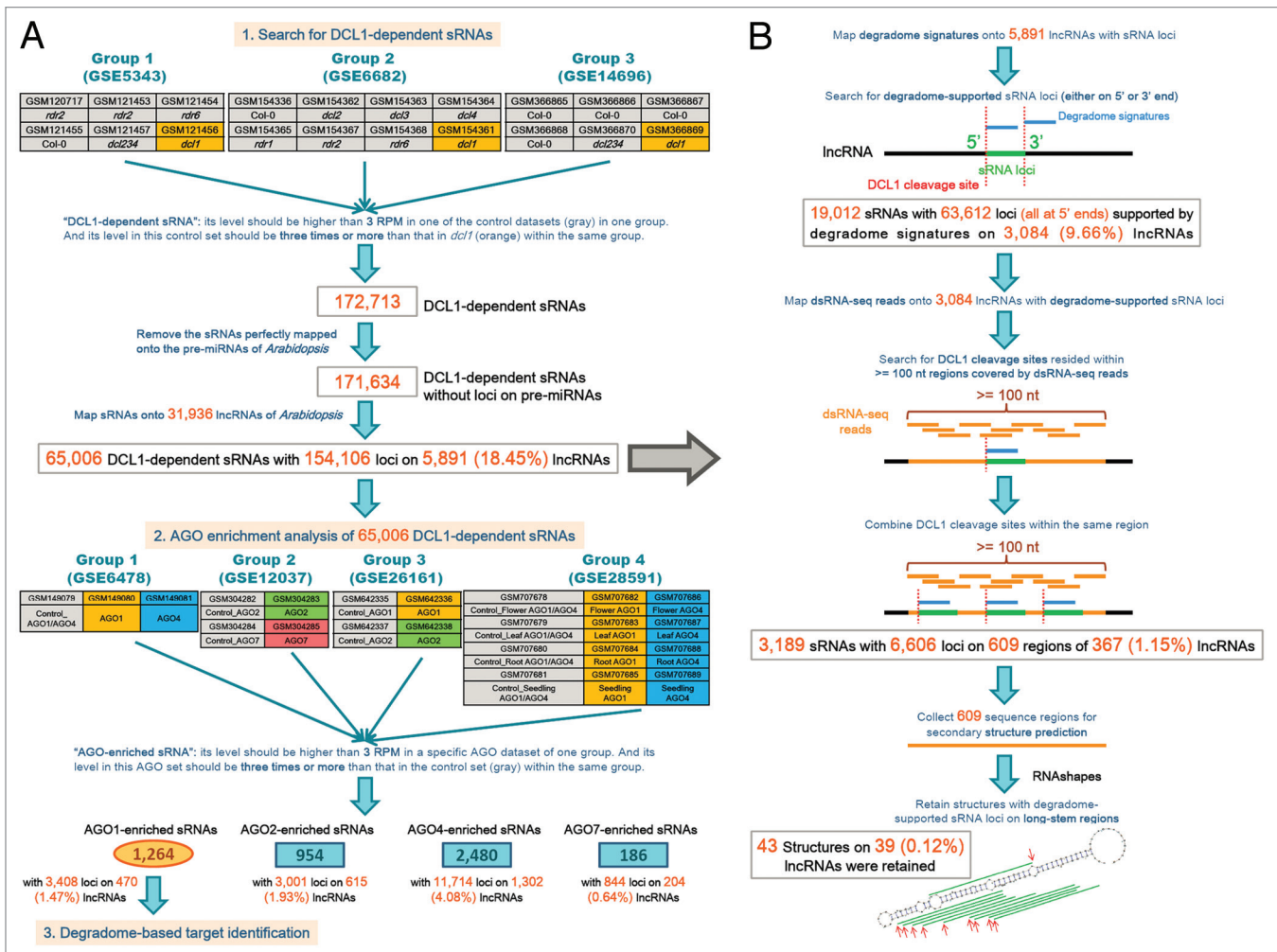


Figure 1. Workflow and result summary of the identification of the DCL1 (Dicer-like 1)-dependent sRNAs (small RNAs) on the long-stem-structured regions of the lncRNAs (long non-coding RNAs) in *Arabidopsis*. (A) Identification of DCL1-dependent sRNAs. Three groups of sRNA high-throughput sequencing (HTS) data sets were used for this study. The “*dcl1*” data sets (highlighted in orange background) were prepared from the *Arabidopsis* mutant *dcl1*. The data sets highlighted in gray background were treated as control sets. For AGO enrichment analysis, four groups of sRNA HTS data sets were utilized, and the data sets highlighted in gray background were treated as control sets. (B) Identification of potential loci of DCL1-dependent sRNAs on the long-stem-structured lncRNAs.

Long non-coding RNAs (lncRNAs), as another part of the “dark matters,” have also been studied. In plants, the lncRNAs are implicated in chromatin modifications and target mimicry (Certain RNA sequences such as lncRNAs possess highly complementary regions which could be recognized by specific miRNAs. However, the RNAs will not be cleaved by the miRNA-associated silencing complexes owing to the existence of mismatches at the position 9th to 11th nucleotide of the miRNAs. Thus, the RNAs serve as decoys to interfere with the binding of the miRNAs to the other genuine target transcripts. This type of inhibitory mechanism of miRNA activities was termed target mimicry in plants.).⁸⁻¹⁰ A recent study reported 6,480 long intergenic non-coding RNAs (lincRNAs) in *Arabidopsis*,¹¹ which have been made available in PLncDB (the plant long non-coding RNA database).¹² On the other hand, the functional significance of the RNA molecules has been suggested to be embedded in the well-organized structures.¹³ Thus, one question was raised

whether these lncRNAs could form internal structures for certain biological outputs, such as sRNA production just like pri-miRNAs.

To this end, we did a comprehensive search for DCL1-dependent sRNAs in *Arabidopsis* by using sRNA HTS data sets prepared from the *dcl1* mutant. As a result, 172,713 DCL1-dependent sRNAs were identified, among which only 1079 could be perfectly mapped onto the registered pre-miRNAs of *Arabidopsis* (miRBase, release 20). This led us to investigate the origination of the remaining large portion of the DCL1-dependent sRNAs. Notably, 65,006 sRNAs could find their loci (a total of 154,106 loci) on 5,891 lncRNAs retrieved from PLncDB. AGO enrichment analysis showed that some of these sRNAs, with distinct sequence characteristics, could be selectively recruited by specific AGO protein complexes. Based on degradome sequencing data, we showed that the DCL1-dependent, AGO1-enriched sRNAs had great potential of

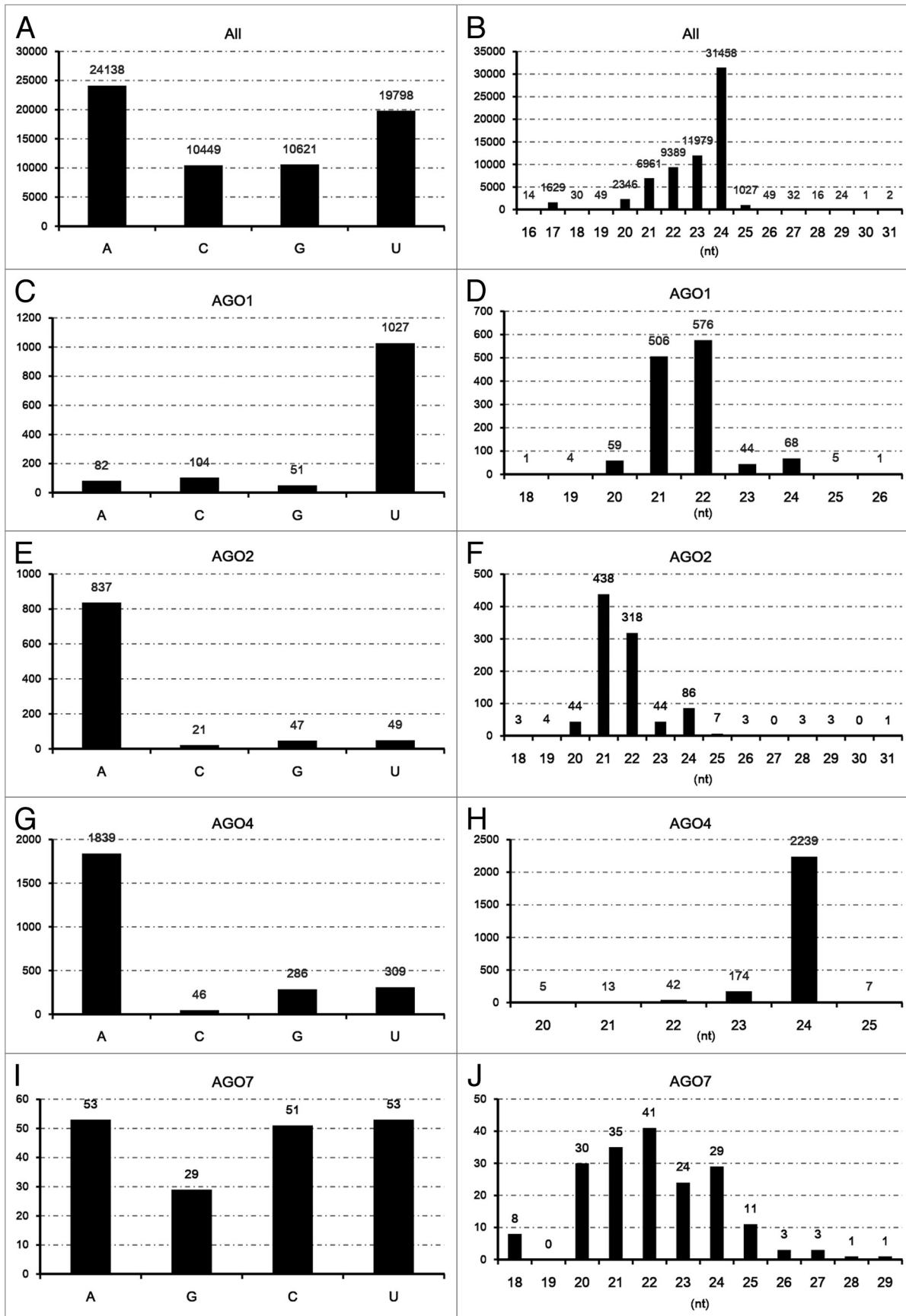


Figure 2. For figure legend see page 376.

Figure 2 (See previous page). Sequence characteristics of the DCL1 (Dicer-like 1)-dependent sRNAs (small RNAs) on the long-stem-structured regions of the lncRNAs (long non-coding RNAs) in *Arabidopsis*. **(A)** 5' terminal composition of all the identified DCL1-dependent sRNAs. **(B)** Sequence length distribution of all the identified DCL1-dependent sRNAs. **(C)** 5' terminal composition of DCL1-dependent, AGO1-enriched sRNAs. **(D)** Sequence length distribution of DCL1-dependent, AGO1-enriched sRNAs. **(E)** 5' terminal composition of DCL1-dependent, AGO2-enriched sRNAs. **(F)** Sequence length distribution of DCL1-dependent, AGO2-enriched sRNAs. **(G)** 5' terminal composition of DCL1-dependent, AGO4-enriched sRNAs. **(H)** Sequence length distribution of DCL1-dependent, AGO4-enriched sRNAs. **(I)** 5' terminal composition of DCL1-dependent, AGO7-enriched sRNAs. **(J)** Sequence length distribution of DCL1-dependent, AGO7-enriched sRNAs.

Table 1. List of genes targeted by Dicer-like 1-dependent, Argonaute 1-enriched small RNAs identified on the long non-coding RNAs of *Arabidopsis*

Small RNA ID	Target transcript	Binding site on target transcript	Cleavage site supported by degradome sequencing data	Target gene	Target gene annotation
DCL1_sRNA13855	AT1G12300.1	1550–1570	1561	AT1G12300	Tetratricopeptide repeat (TPR)-like superfamily protein
DCL1_sRNA13839	AT1G12300.1	1551–1571	1562		
DCL1_sRNA13855	AT1G12620.1	1706–1726	1717	AT1G12620	Pentatricopeptide repeat (PPR) superfamily protein
DCL1_sRNA13839	AT1G12620.1	1707–1727	1718		
DCL1_sRNA13855	AT1G12700.1	1503–1523	1512	AT1G12700	RNA PROCESSING FACTOR 1 (RPF1)
DCL1_sRNA13855	AT1G12775.1	1502–1522	1514	AT1G12775	Pentatricopeptide repeat (PPR) superfamily protein
DCL1_sRNA13839	AT1G12775.1	1503–1523			
DCL1_sRNA5687	AT1G16890.1	618–638	627	AT1G16890	UBC36/UBC13B encodes a protein that may play a role in DNA damage responses and error-free post-replicative DNA repair
DCL1_sRNA5409	AT1G16890.1	617–638			
DCL1_sRNA5987	AT1G16890.1	615–636			
DCL1_sRNA5300	AT1G16890.1	616–637			
DCL1_sRNA5729	AT1G16890.1	617–637			
DCL1_sRNA5687	AT1G16890.2	637–657	646		
DCL1_sRNA5409	AT1G16890.2	636–657			
DCL1_sRNA5987	AT1G16890.2	634–655			
DCL1_sRNA5300	AT1G16890.2	635–656			
DCL1_sRNA5729	AT1G16890.2	636–656			
DCL1_sRNA5687	AT1G16890.3	664–684	673		
DCL1_sRNA5409	AT1G16890.3	663–684			
DCL1_sRNA5987	AT1G16890.3	661–682			
DCL1_sRNA5300	AT1G16890.3	662–683			
DCL1_sRNA5729	AT1G16890.3	663–683			
DCL1_sRNA36672	AT1G27250.1	347–368	360	AT1G27250	Paired amphipathic helix (PAH2) superfamily protein
DCL1_sRNA64198	AT1G31020.1	654–674	665	AT1G31020	Thioredoxin O2 (TO2)
DCL1_sRNA5018	AT1G45688.1	26–47	36	AT1G45688	Unknown protein
DCL1_sRNA5018	AT1G45688.2	12–33	22		
DCL1_sRNA25197	AT1G56110.1	1534–1554	1545	AT1G56110	NOP56-like protein
DCL1_sRNA14038	AT1G58400.1	2646–2667	2658	AT1G58400	Disease resistance protein (CC-NBS-LRR class) family
DCL1_sRNA14056	AT1G58400.1	2645–2666			
DCL1_sRNA6150	AT1G59830.1	1230–1250	1239	AT1G59830	Encodes one of the isoforms of the catalytic subunit of protein phosphatase 2A
DCL1_sRNA6150	AT1G59830.2	1319–1339	1328		
DCL1_sRNA13855	AT1G62860.1	1492–1512	1503	AT1G62860	Pseudogene of pentatricopeptide (PPR) repeat-containing protein
DCL1_sRNA13839	AT1G62860.1	1493–1513	1504		
DCL1_sRNA13841	AT1G62910.1	535–555	547	AT1G62910	Pentatricopeptide repeat (PPR) superfamily protein
DCL1_sRNA13811	AT1G62910.1	535–556			

Table 1. List of genes targeted by Dicer-like 1-dependent, Argonaute 1-enriched small RNAs identified on the long non-coding RNAs of *Arabidopsis* (continued)

Small RNA ID	Target transcript	Binding site on target transcript	Cleavage site supported by degradome sequencing data	Target gene	Target gene annotation
DCL1_sRNA13841	AT1G62914.1	517–537	529	AT1G62914	Pentatricopeptide (PPR) repeat-containing protein
DCL1_sRNA13811	AT1G62914.1	517–538			
DCL1_sRNA13922	AT1G62930.1	1458–1478	1469	AT1G62930	RPF3 encodes a pentatricopeptide repeat (PPR) protein involved in 5' processing of different mitochondrial mRNAs
DCL1_sRNA13817	AT1G62930.1	1457–1477			
DCL1_sRNA13816	AT1G62930.1				
DCL1_sRNA13922	AT1G63080.1	1501–1521	1512	AT1G63080	Transacting siRNA generating locus
DCL1_sRNA13816	AT1G63080.1	1500–1520			
DCL1_sRNA13841	AT1G63130.1	650–670	662	AT1G63130	Transacting siRNA generating locus
DCL1_sRNA13811	AT1G63130.1	650–671			
DCL1_sRNA13841	AT1G63150.1	535–555	547	AT1G63150	Transacting siRNA generating locus
DCL1_sRNA13811	AT1G63150.1	535–556			
DCL1_sRNA13829	AT1G63230.1	1230–1251	1242	AT1G63230	Tetratricopeptide repeat (TPR)-like superfamily protein
DCL1_sRNA13800	AT1G63230.1	1230–1250			
DCL1_sRNA13829	AT1G63630.1	542–563	554	AT1G63630	Tetratricopeptide repeat (TPR)-like superfamily protein
DCL1_sRNA13800	AT1G63630.1	542–562			
DCL1_sRNA13829	AT1G63630.2	591–612			
DCL1_sRNA13800	AT1G63630.2	591–611	603		
DCL1_sRNA5518	AT1G64720.1	1139–1161	1151	AT1G64720	Membrane related protein CP5
DCL1_sRNA6493	AT1G64720.1	1138–1159	1150		
DCL1_sRNA5389	AT1G64720.1	1140–1161	1151		
DCL1_sRNA4887	AT1G64720.1	1141–1161	1151		
DCL1_sRNA5993	AT1G72050.1	1293–1314	1304	AT1G72050	Encodes a transcriptional factor TFIIIA required for transcription of 5S rRNA gene
DCL1_sRNA5733	AT1G72050.1	1293–1313			
DCL1_sRNA5031	AT1G72050.1	1292–1313			
DCL1_sRNA5993	AT1G72050.2	1060–1081	1071		
DCL1_sRNA5733	AT1G72050.2	1060–1080			
DCL1_sRNA5031	AT1G72050.2	1059–1080			
DCL1_sRNA46232	AT1G73500.1	127–149	140	AT1G73500	Member of MAP Kinase Kinase family
DCL1_sRNA5231	AT1G75220.1	1802–1823	1815	AT1G75220	Encodes a vacuolar glucose exporter
DCL1_sRNA64537	AT2G01010.1	1649–1669	1661	AT2G01010	18SrRNA
DCL1_sRNA3154	AT2G12440.1	4625–4648	4640	AT2G12440	Transposable element gene
DCL1_sRNA1263	AT2G12440.1	4629–4648			
DCL1_sRNA1141	AT2G17442.1	672–695	687	AT2G17442	Unknown protein
DCL1_sRNA1141	AT2G17442.2	696–719	711		
DCL1_sRNA1141	AT2G17442.3	693–716	708		
DCL1_sRNA1141	AT2G17442.4	645–668	660		
DCL1_sRNA1141	AT2G17442.5	644–667	659		
DCL1_sRNA31206	AT2G27740.1	20–43	32	AT2G27740	Family of unknown function (DUF662)
DCL1_sRNA5477	AT2G28350.1	2179–2200	2192	AT2G28350	AUXIN RESPONSE FACTOR 10 (ARF10), involved in root cap cell differentiation

Table 1. List of genes targeted by Dicer-like 1-dependent, Argonaute 1-enriched small RNAs identified on the long non-coding RNAs of *Arabidopsis* (continued)

Small RNA ID	Target transcript	Binding site on target transcript	Cleavage site supported by degradome sequencing data	Target gene	Target gene annotation
DCL1_sRNA26509	AT2G28550.1	1558–1577	1568	AT2G28550	Related to AP2.7 (RAP2.7)
DCL1_sRNA26510	AT2G28550.1	1556–1577			
DCL1_sRNA26509	AT2G28550.2	1630–1649	1640		
DCL1_sRNA26510	AT2G28550.2	1628–1649			
DCL1_sRNA26509	AT2G28550.3	1603–1622	1613		
DCL1_sRNA26510	AT2G28550.3	1601–1622			
DCL1_sRNA62245	AT2G33860.1	1673–1693/1793–1813	1685/1804	AT2G33860	ETTIN (ETT)
DCL1_sRNA62203	AT2G33860.1	1673–1694/1793–1814	1686/1805		
DCL1_sRNA62205	AT2G33860.1	1674–1694/1794–1814	1686/1805		
DCL1_sRNA62234	AT2G33860.1	1674–1694/1794–1814	1686/1805		
DCL1_sRNA62237	AT2G33860.1	1675–1694/1795–1814	1686/1805		
DCL1_sRNA62218	AT2G33860.1	1675–1695/1795–1815	1686/1805		
DCL1_sRNA62198	AT2G33860.1	1675–1695/1795–1815	1686/1805		
DCL1_sRNA24900	AT2G33860.1	1676–1696/1796–1816	1686/1805		
DCL1_sRNA57442	AT2G35430.1	844–865	854		
DCL1_sRNA7007	AT2G36380.1	4448–4469	4461	AT2G36380	Pleiotropic drug resistance 6 (PDR6)
DCL1_sRNA6129	AT2G37370.1	1365–1386	1378	AT2G37370	Unknown protein
DCL1_sRNA3463	AT2G37370.1	1419–1438	1427		
DCL1_sRNA31206	AT2G37890.1	1447–1470	1461	AT2G37890	Mitochondrial substrate carrier family protein
DCL1_sRNA13846	AT2G39681.1	724–744	735	AT2G39681	Trans-acting siRNA primary transcript
DCL1_sRNA10442	AT2G39681.1	724–744			
DCL1_sRNA13822	AT2G39681.1	585–606	597		
DCL1_sRNA13851	AT2G39681.1	585–605			
DCL1_sRNA13822	AT2G41950.1	422–443	434	AT2G41950	Unknown protein
DCL1_sRNA13851	AT2G41950.1	422–442	434		
DCL1_sRNA6760	AT2G47160.1	2252–2273	2262	AT2G47160	Boron transporter
DCL1_sRNA6760	AT2G47160.2	2331–2352	2341		
DCL1_sRNA4906	AT3G03040.1	1099–1120	1109	AT3G03040	F-box/RNI-like superfamily protein
DCL1_sRNA4946	AT3G03040.1	1098–1118			

Table 1. List of genes targeted by Dicer-like 1-dependent, Argonaute 1-enriched small RNAs identified on the long non-coding RNAs of *Arabidopsis* (continued)

Small RNA ID	Target transcript	Binding site on target transcript	Cleavage site supported by degradome sequencing data	Target gene	Target gene annotation
DCL1_sRNA9465	AT3G04730.1	752–773	762	AT3G04730	INDOLEACETIC ACID-INDUCED PROTEIN 16 (IAA16)
DCL1_sRNA62220	AT3G05340.1	2296–2318	2310	AT3G05340	Tetratricopeptide repeat (TPR)-like superfamily protein
DCL1_sRNA62220	AT3G05345.1	19–41	33	AT3G05345	Chaperone DnaJ-domain superfamily protein
DCL1_sRNA5844	AT3G05590.1	740–761	753	AT3G05590	RIBOSOMAL PROTEIN L18 (RPL18)
DCL1_sRNA13818	AT3G15605.1	1791–1811	1803	AT3G15605	Nucleic acid binding
DCL1_sRNA13818	AT3G15605.2	1785–1805	1797		
DCL1_sRNA13818	AT3G15605.3	1608–1628	1620		
DCL1_sRNA13818	AT3G15605.4	1540–1560	1552		
DCL1_sRNA4896	AT3G22010.1	715–735	726	AT3G22010	Receptor-like protein kinase-related family protein
DCL1_sRNA5080	AT3G22990.1	877–900	890	AT3G22990	LEAF AND FLOWER RELATED (LFR)
DCL1_sRNA5467	AT3G23000.1	1138–1159	1148	AT3G23000	CBL-INTERACTING PROTEIN KINASE 7 (CIPK7)
DCL1_sRNA30437	AT3G25470.1	1095–1118	1110	AT3G25470	Bacterial hemolysin-related
DCL1_sRNA64537	AT3G41768.1	1649–1669	1661	AT3G41768	18SrRNA
DCL1_sRNA4900	AT3G44310.1	757–777	768	AT3G44310	NITRILASE 1 (NIT1)
DCL1_sRNA4900	AT3G44310.2	639–659	650		
DCL1_sRNA4900	AT3G44310.3	757–777	768		
DCL1_sRNA26509	AT3G54990.1	965–985	976	AT3G54990	Encodes a AP2 domain transcription factor that can repress flowering
DCL1_sRNA22374	AT3G54990.1				
DCL1_sRNA26510	AT3G54990.1				
DCL1_sRNA6738	AT3G56730.1	605–625	616	AT3G56730	Putative endonuclease or glycosyl hydrolase
DCL1_sRNA6738	AT3G56730.2	660–680	671		
DCL1_sRNA31732	AT4G06708.1	15–38	28	AT4G06708	Transposable element gene
DCL1_sRNA6150	AT4G12730.1	1364–1384	1376	AT4G12730	FASCICLIN-LIKE ARABINO GALACTAN 2 (FLA2)
DCL1_sRNA7163	AT4G15830.1	855–876	868	AT4G15830	ARM repeat superfamily protein
DCL1_sRNA47338	AT4G16830.1	119–139	130	AT4G16830	Hyaluronan/mRNA binding family
DCL1_sRNA47338	AT4G16830.2	95–115	106		
DCL1_sRNA47338	AT4G16830.3	119–139	130		

performing target cleavages. To find further evidences to support the origination of the DCL1-dependent sRNAs from lncRNAs, we searched for the degradome-based cleavage signals at either ends of the sRNA loci, which were supposed to be produced during DCL1-mediated processing of the long-stem structures. As a result, 63612 loci belonging to 19012 sRNAs were supported by degradome signatures. Among these loci, 6606 reside within 609 regions of 100 nt or longer. Intriguingly, all of these regions are covered by dsRNA-seq (double-stranded RNA sequencing) reads, indicating their great potential of forming long-stem structures in vivo. Thus, these regions were subjected to secondary structure prediction. After manual screening for the long-stem structures with degradome-supported sRNA loci, 43 structures on 39 lncRNAs were obtained. Taken together, our results present a DCL1-dependent biogenesis pathway for the

lncRNA-originated sRNAs with potential regulatory activities. We hope that the proposed model could inspire more research efforts to study on the biological roles of lncRNAs in plants.

Results and Discussion

Identification of DCL1-dependent sRNAs potentially originated from lncRNAs

Three groups of sRNA HTS data (GSE5343, GSE6682 and GSE14696) were included, and were analyzed separately (Fig. 1A). For the three groups, in addition to the data sets prepared from the wild type plants of *Arabidopsis*, the data sets prepared from the mutants *rdrl*, *rdr2*, *rdr6*, *dcl2*, *dcl3*, *dcl4*, and *dcl234* (triple mutant) were also recruited as the control sets to

Table 1. List of genes targeted by Dicer-like 1-dependent, Argonaute 1-enriched small RNAs identified on the long non-coding RNAs of *Arabidopsis* (continued)

Small RNA ID	Target transcript	Binding site on target transcript	Cleavage site supported by degradome sequencing data	Target gene	Target gene annotation
DCL1_sRNA15973	AT4G18120.1	2301–2322	2314	AT4G18120	MEI2-LIKE 3 (ML3)
DCL1_sRNA15973	AT4G18120.2	2152–2173	2165		
DCL1_sRNA7119	AT4G23450.2	180–201	192	AT4G23450	ABA INSENSITIVE RING PROTEIN 1 (AIRP1)
DCL1_sRNA17116	AT4G29770.1	728–748	739	AT4G29770	Target of trans acting-siR480/255
DCL1_sRNA61901	AT4G29770.1	726–747			
DCL1_sRNA61963	AT4G29770.1	728–748			
DCL1_sRNA17095	AT4G29770.1	728–748			
DCL1_sRNA17297	AT4G29770.1	729–748			
DCL1_sRNA17118	AT4G29770.1	728–748			
DCL1_sRNA61866	AT4G29770.1	727–748			
DCL1_sRNA17098	AT4G29770.1	729–748			
DCL1_sRNA61962	AT4G29770.1	728–748			
DCL1_sRNA61865	AT4G29770.1	728–748			
DCL1_sRNA17097	AT4G29770.1	731–748			
DCL1_sRNA61867	AT4G29770.1	729–748			
DCL1_sRNA17116	AT4G29770.2	770–790			
DCL1_sRNA61901	AT4G29770.2	768–789			
DCL1_sRNA61963	AT4G29770.2	770–790			
DCL1_sRNA17095	AT4G29770.2	770–790	781	AT4G29770	Target of trans acting-siR480/255
DCL1_sRNA17297	AT4G29770.2	771–790			
DCL1_sRNA17118	AT4G29770.2	770–790			
DCL1_sRNA61866	AT4G29770.2	769–790			
DCL1_sRNA17098	AT4G29770.2	771–790			
DCL1_sRNA61962	AT4G29770.2	770–790			
DCL1_sRNA61865	AT4G29770.2	770–790			
DCL1_sRNA17097	AT4G29770.2	773–790			
DCL1_sRNA61867	AT4G29770.2	771–790			
DCL1_sRNA7075	AT4G33280.1	808–829			
DCL1_sRNA26509	AT4G36920.1	1329–1349	1340	AT4G36920	APETALA 2 (AP2)
DCL1_sRNA22374	AT4G36920.1				
DCL1_sRNA26510	AT4G36920.1	1328–1349	1304	AT4G36920	APETALA 2 (AP2)
DCL1_sRNA26509	AT4G36920.2	1293–1313			
DCL1_sRNA22374	AT4G36920.2				
DCL1_sRNA26510	AT4G36920.2	1292–1313			
DCL1_sRNA22374	AT5G04275.1	1–21	12	AT5G04275	MICRORNA172B (MIR172B), a microRNA that targets several genes containing AP2 domains
DCL1_sRNA12080	AT5G08590.1	34–56	48	AT5G08590	SNF1-RELATED PROTEIN KINASE 2.1 (SNRK2.1)
DCL1_sRNA10500	AT5G11660.1	803–824	815	AT5G11660	Protein of Unknown Function (DUF239)
DCL1_sRNA7229	AT5G13800.1	1654–1675	1667	AT5G13800	PHEOPHYTINASE (PPH)
DCL1_sRNA5234	AT5G14565.1	1896–1916	1907	AT5G14565	MICRORNA398C (MIR398C)

Table 1. List of genes targeted by Dicer-like 1-dependent, Argonaute 1-enriched small RNAs identified on the long non-coding RNAs of *Arabidopsis* (continued)

Small RNA ID	Target transcript	Binding site on target transcript	Cleavage site supported by degradome sequencing data	Target gene	Target gene annotation
DCL1_sRNA13841	AT5G16640.1	581–601	593	AT5G16640	Pentatricopeptide repeat (PPR) superfamily protein
DCL1_sRNA13811	AT5G16640.1	581–602	593		
DCL1_sRNA6198	AT5G16800.1	1222–1242	1233	AT5G16800	Acyl-CoA N-acyltransferases (NAT) superfamily protein
DCL1_sRNA6198	AT5G16800.2	1139–1159	1150		
DCL1_sRNA6198	AT5G16800.3	1148–1168	1159		
DCL1_sRNA17116	AT5G18040.1	675–695	686	AT5G18040	Unknown protein
DCL1_sRNA61901	AT5G18040.1	672–694			
DCL1_sRNA17095	AT5G18040.1	675–695			
DCL1_sRNA17297	AT5G18040.1	676–695			
DCL1_sRNA17118	AT5G18040.1	675–695			
DCL1_sRNA61866	AT5G18040.1	674–695			
DCL1_sRNA17098	AT5G18040.1	676–695			
DCL1_sRNA61865	AT5G18040.1	675–695			
DCL1_sRNA17097	AT5G18040.1	678–695			
DCL1_sRNA61867	AT5G18040.1	676–695			

do a more comprehensive search for DCL1-dependent sRNAs. It was based on the consideration that the activity of DCL1 is not attenuated in above mutants. For each group, a DCL1-dependent sRNA was defined as follows: its accumulation level should be 3 RPM (reads per million) or higher in at least one of the control sets; and its level in this control set should be three times or more than that in the *dcl1* data set within the same group. A rigorous sequence search was performed, and sequence mismatches and length variations were not allowed. In other words, two types of DCL1-dependent sRNAs will be uncovered: (1) the accumulation level of the DCL1-dependent sRNA is 3 RPM or higher in one of the control set, and the exact sequence does not exist in the *dcl1* data set within the same group; (2) the exact sequence of DCL1-dependent sRNA exists in both the control set and the *dcl1* set within the same group; however, its accumulation level is 3 RPM or higher in the control set, and is three times or more than that in the *dcl1* data set. As a result, 172 713 DCL1-dependent sRNAs were identified. Since the research focus of this study is on the lncRNA-originated sRNAs, but not the miRNAs or the byproducts from miRNA precursors, all the DCL1-dependent sRNAs were mapped to all of the registered pre-miRNAs of *Arabidopsis* (miRBase, release 20), and those have perfect loci on the pre-miRNAs were removed. Interestingly, a dominant portion of the DCL1-dependent sRNAs (a total of 171 634) was retained (Data S1). Then, all of these DCL1-dependent sRNAs were mapped to the *Arabidopsis* lncRNAs retrieved from PLncDB.¹² Notably, 65 006 sRNAs (Data S2) could find their loci (a total of 154 106 loci) on 5891 lncRNAs (Fig. 1A). To date, 3' modifications (e.g., adenylation and uridylation) of mature miRNAs have been

widely observed in both animals and plants.^{14,15} To exclude the possibility that the DCL1-dependent sRNAs without perfect loci on the *Arabidopsis* pre-miRNAs was contributed by 3' end modifications, a systemic search for the 3' modified candidates of the miRNAs was performed. However, only two DCL1-dependent sRNAs “AGAGGUGACC AUUGGAGAUG G” and “AGGCUUUUAA GAUCUGGUUG CGGU” were identified to contain but be longer than the miRNAs ath-miR5662 and ath-miR5643a/b. Together, our results indicate that lncRNAs are a potentially great contributor for the biogenesis of DCL1-dependent sRNAs in *Arabidopsis*.

AGO enrichment analysis

According to the current model,^{6,7,16,17} incorporation into specific AGO silencing complexes is a prerequisite for the action of miRNAs and other sRNAs. In this regard, AGO enrichment analysis was performed for the 65,006 DCL1-dependent sRNAs identified on the lncRNAs. Four groups of AGO-associated sRNA HTS data sets were included in this analysis, and were treated separately (Fig. 1A). For each group, a sRNA enriched in a specific AGO protein complex was defined as follows: its level in a specific AGO data set should be 3 RPM or higher; and its level in this AGO data set should be three times or more than that in the control set. As a result, 1264 DCL1-dependent sRNAs showed high enrichment in AGO1 complexes (Data S3), and 954, 2480, and 186 sRNAs were enriched in AGO2, AGO4 and AGO7 respectively (Data S4).

Next, the sequence characteristics of these AGO-enriched sRNAs were analyzed. For all the 65 006 DCL1-dependent sRNAs identified on the lncRNAs, slight enrichment was observed for 5' A- and 5' U-started sRNAs (Fig. 2A). However,

Table 1. List of genes targeted by Dicer-like 1-dependent, Argonaute 1-enriched small RNAs identified on the long non-coding RNAs of *Arabidopsis* (continued)

Small RNA ID	Target transcript	Binding site on target transcript	Cleavage site supported by degradome sequencing data	Target gene	Target gene annotation
DCL1_sRNA17116	AT5G18065.1	726–746	737	AT5G18065	Unknown protein
DCL1_sRNA61901	AT5G18065.1	723–745			
DCL1_sRNA17095	AT5G18065.1	726–746			
DCL1_sRNA17297	AT5G18065.1	727–746			
DCL1_sRNA17118	AT5G18065.1	726–746			
DCL1_sRNA61866	AT5G18065.1	725–746			
DCL1_sRNA17098	AT5G18065.1	727–746			
DCL1_sRNA61865	AT5G18065.1	726–746			
DCL1_sRNA17097	AT5G18065.1	729–746			
DCL1_sRNA61867	AT5G18065.1	727–746			
DCL1_sRNA6188	AT5G33406.1	1505–1525	1517	AT5G33406	hAT dimerization domain-containing protein/transposase-related
DCL1_sRNA59503	AT5G40810.1	1015–1038	1027	AT5G40810	Cytochrome C1 family
DCL1_sRNA59503	AT5G40810.2	1344–1367	1356		
DCL1_sRNA7136	AT5G51300.1	2469–2488	2477	AT5G51300	Splicing factor-related
DCL1_sRNA6885	AT5G51300.1	2468–2488			
DCL1_sRNA5824	AT5G59732.1	1537–1558	1548	AT5G59732	Potential natural antisense gene, locus overlaps with AT5G59730

it is quite different for the AGO-enriched sRNAs. The AGO1-enriched sRNAs dominantly begin with U (Fig. 2C), and the AGO2- and AGO4-enriched ones mainly start with A (Fig. 2E and G). No obvious bias of the 5' terminal nucleotide composition was observed for the sRNAs enriched in AGO7 (Fig. 2I). For sequence length distribution, a dominant portion of the 65 006 DCL1-dependent sRNAs is enriched in 21 to 24 nt, especially in 24 nt (Fig. 2B). For both the AGO1-enriched and the AGO2-enriched sRNAs, most of the sRNAs are 21 to 22 nt in length (Fig. 2D and F). The AGO4-enriched sRNAs are dominantly 24 nt (Fig. 2H), and the AGO7-enriched ones dominantly range from 20 to 24 nt (Fig. 2J). The above described sequence characteristics of the AGO-enriched sRNAs correlate well with the previously reported sequence features of the AGO1-, AGO2- and AGO4-associated sRNAs in *Arabidopsis*.¹⁸

Target identification for the DCL1-dependent, AGO1-enriched sRNAs

Among the diverse AGO proteins, AGO1 was well characterized to possess RNA slicer activity.¹⁷ Thus, the sRNAs associated with AGO1 silencing complexes are likely to guide transcript cleavage-based target gene regulation in plants, which is similar to the action of miRNAs.^{6,7} In this consideration, a large-scale target identification of the 1,264 DCL1-dependent, AGO1-enriched sRNAs was performed. First, all of the TAIR (The *Arabidopsis* Information Resource; release 10)-annotated gene transcripts were included as the database for target

binding site search by using miRU algorithm^{19,20} with default parameters. Then, the predicted target transcripts were validated based on degradome sequencing data (see details in “Materials and Methods”). Considering the fact that some evident cleavage signals out of the canonical slicing sites (10th to 11th nt of the regulatory sRNAs) were detected in the previous experiments,^{21–24} the binding sites with prominent slicing signals resided within 8th to 12th nt of the sRNAs were retained. As a result, 109 transcripts encoded by 78 genes were validated to be targeted by 96 sRNAs, resulting in 248 sRNA—target pairs (Table 1; Fig. S1). Notably, in many cases, the cleavage-based regulation of the targets was supported by evident degradome signatures resided within 9th to 11th nt of the sRNAs (Fig. 3; Fig. S2), indicating the similarity of the action modes between the DCL1-dependent, AGO1-enriched sRNAs and the plant miRNAs. Besides, certain transcripts possess two binding sites which were simultaneously targeted by specific sRNAs. For example, AT2G39681.1 has two binding sites (i.e., 585th to 606th nt and 724th to 744th nt) which were targeted by DCL1_sRNA13822 and DCL1_sRNA13851, and DCL1_sRNA10442 and DCL1_sRNA13846 respectively (Fig. 3). More interestingly, 44 lncRNAs were uncovered to be targeted by 23 sRNAs, resulting in a total of 64 sRNA—target pairs (Fig. S3). Quite prominent cleavage signals were observed within the binding sites on several lncRNAs (Fig. 4). Thus, it raises the possibility that in plants, certain lncRNAs might serve as the precursors for sRNA generation which some

Table 1. List of genes targeted by Dicer-like 1-dependent, Argonaute 1-enriched small RNAs identified on the long non-coding RNAs of *Arabidopsis* (continued)

Small RNA ID	Target transcript	Binding site on target transcript	Cleavage site supported by degradome sequencing data	Target gene	Target gene annotation
DCL1_sRNA26509	AT5G60120.1	1647–1667	1658	AT5G60120	TARGET OF EARLY ACTIVATION TAGGED 2 (TOE2)
DCL1_sRNA22374	AT5G60120.1				
DCL1_sRNA26510	AT5G60120.1				
DCL1_sRNA26509	AT5G60120.2	1810–1830	1821		
DCL1_sRNA22374	AT5G60120.2				
DCL1_sRNA26510	AT5G60120.2				
DCL1_sRNA62203	AT5G60450.1	1873–1894/2083–2104	1885/2095	AT5G60450	AUXIN RESPONSE FACTOR 4 (ARF4)
DCL1_sRNA62218	AT5G60450.1	1875–1895/2085–2105			
DCL1_sRNA24900	AT5G60450.1	1876–1896/2086–2106			
DCL1_sRNA62205	AT5G60450.1	1874–1894/2084–2104			
DCL1_sRNA62237	AT5G60450.1	1875–1894/2085–2104			
DCL1_sRNA62234	AT5G60450.1	1874–1894/2084–2104			
DCL1_sRNA62245	AT5G60450.1	1873–1893/2083–2103			
DCL1_sRNA62198	AT5G60450.1	1875–1895/2085–2105			

other lncRNAs might be treated as the targets of the lncRNA-originated sRNAs.

Biological hints inferred from certain sRNA—Target pairs

Certain regulatory networks constituted by dozens of degradome-validated sRNA—target pairs were present here, since some biological implications were obtained based on the target gene annotations (TAIR, release 10) and the analytical results from PlantGSEA (The Plant GeneSet Enrichment Analysis Toolkit; <http://structuralbiology.cau.edu.cn/PlantGSEA/analysis.php>).²⁵ Within the network shown in **Figure 5A**, *AT2G28550*, *AT3G54990*, *AT4G33280*, *AT4G36920* and *AT5G60120* were annotated to be the members of *APETALA2* (*AP2*) family, which were potentially involved in flower development.^{26–28} Two other target genes, *AT2G33860* and *AT3G22990*, were also involved in flower development according to the TAIR annotations. More interestingly, *AT5G04275* encoding *MIR172B* was targeted by DCL1_sRNA22374. miR172 has been demonstrated to play an important role in floral organ development in *Arabidopsis*.^{29,30}

Based on the above results, a regulatory cascade implicated in flower development, DCL1-dependent sRNA—*MIR172*—*AP2*, was proposed (**Fig. 5A**). For the second network shown in **Figure 5B**, all of the six target genes are functionally related to RNAs based on TAIR annotations. *AT1G72050* encodes a transcription factor TFIIA required for the transcription of 5S rRNA (rRNA) gene, and *AT2G01010* and *AT3G41768* encode 18S rRNA. *AT2G39681* encodes a primary transcript for *trans*-acting siRNA (small interfering RNA) production, and *AT5G59732* is a potential natural antisense gene overlapping with *AT5G59730*. Besides, *AT5G51300* is involved in RNA splicing. The third network is involved in auxin signaling (**Fig. 5C**). *AT2G28350* encodes ARF10 (Auxin Response Factor 10) involved in root cap formation,³¹ and *AT5G60450* and *AT5G62000* encode ARF4 and ARF2 respectively. *AT3G04730* encodes IAA16 (indoleacetic acid-induced protein 16) which is also implicated in auxin signal transduction. Based on the analytical results of PlantGSEA,²⁵ certain literature-based evidences were obtained to support

Table 1. List of genes targeted by Dicer-like 1-dependent, Argonaute 1-enriched small RNAs identified on the long non-coding RNAs of *Arabidopsis* (continued)

Small RNA ID	Target transcript	Binding site on target transcript	Cleavage site supported by degradome sequencing data	Target gene	Target gene annotation
DCL1_sRNA62203	AT5G62000.1	1836–1857	1848	AT5G62000	AUXIN RESPONSE FACTOR 2 (ARF2)
DCL1_sRNA62218	AT5G62000.1	1838–1858			
DCL1_sRNA24900	AT5G62000.1	1839–1859			
DCL1_sRNA62205	AT5G62000.1	1837–1857			
DCL1_sRNA62237	AT5G62000.1	1838–1857			
DCL1_sRNA62234	AT5G62000.1	1837–1857			
DCL1_sRNA62245	AT5G62000.1	1836–1856			
DCL1_sRNA62198	AT5G62000.1	1838–1858			
DCL1_sRNA62203	AT5G62000.2	1734–1755	1746		
DCL1_sRNA62218	AT5G62000.2	1736–1756			
DCL1_sRNA24900	AT5G62000.2	1737–1757			
DCL1_sRNA62205	AT5G62000.2	1735–1755			
DCL1_sRNA62237	AT5G62000.2	1736–1755			
DCL1_sRNA62234	AT5G62000.2	1735–1755			
DCL1_sRNA62245	AT5G62000.2	1734–1754			
DCL1_sRNA62198	AT5G62000.2	1736–1756			
DCL1_sRNA62203	AT5G62000.3	1734–1755	1746		
DCL1_sRNA62218	AT5G62000.3	1736–1756			
DCL1_sRNA24900	AT5G62000.3	1737–1757			
DCL1_sRNA62205	AT5G62000.3	1735–1755			
DCL1_sRNA62237	AT5G62000.3	1736–1755			
DCL1_sRNA62234	AT5G62000.3	1735–1755			
DCL1_sRNA62245	AT5G62000.3	1734–1754			
DCL1_sRNA62198	AT5G62000.3	1736–1756			
DCL1_sRNA62203	AT5G62000.4	1734–1755	1746		
DCL1_sRNA62218	AT5G62000.4	1736–1756			
DCL1_sRNA24900	AT5G62000.4	1737–1757			
DCL1_sRNA62205	AT5G62000.4	1735–1755			
DCL1_sRNA62237	AT5G62000.4	1736–1755			
DCL1_sRNA62234	AT5G62000.4	1735–1755			
DCL1_sRNA62245	AT5G62000.4	1734–1754			
DCL1_sRNA62198	AT5G62000.4	1736–1756			
DCL1_sRNA26509	AT5G67180.1	1297–1318	1309	AT5G67180	TARGET OF EARLY ACTIVATION TAGGED 3 (TOE3)
DCL1_sRNA26510	AT5G67180.1	1296–1318			

Please refer to **Figure S2** for degradome sequencing data-based cleavage evidences.

some of the sRNA—target pairs whose interactions could be significantly influenced by the activity of DCL1. The 12 target genes (*AT1G62910*, *AT1G62930*, *AT1G63080*, *AT1G63130*, *AT2G28350*, *AT2G33860*, *AT4G29770*, *AT4G36920*, *AT5G18040*, *AT5G60120*, *AT5G60450* and *AT5G67180*) shown

in **Figure 5D** were significantly upregulated in the *dcl1* mutant relative to the wild type plants of *Arabidopsis*.^{32,33} On the other hand, the above information partially supports the interactions between the 12 target genes and the corresponding DCL1-dependent sRNAs (**Fig. 5D**).

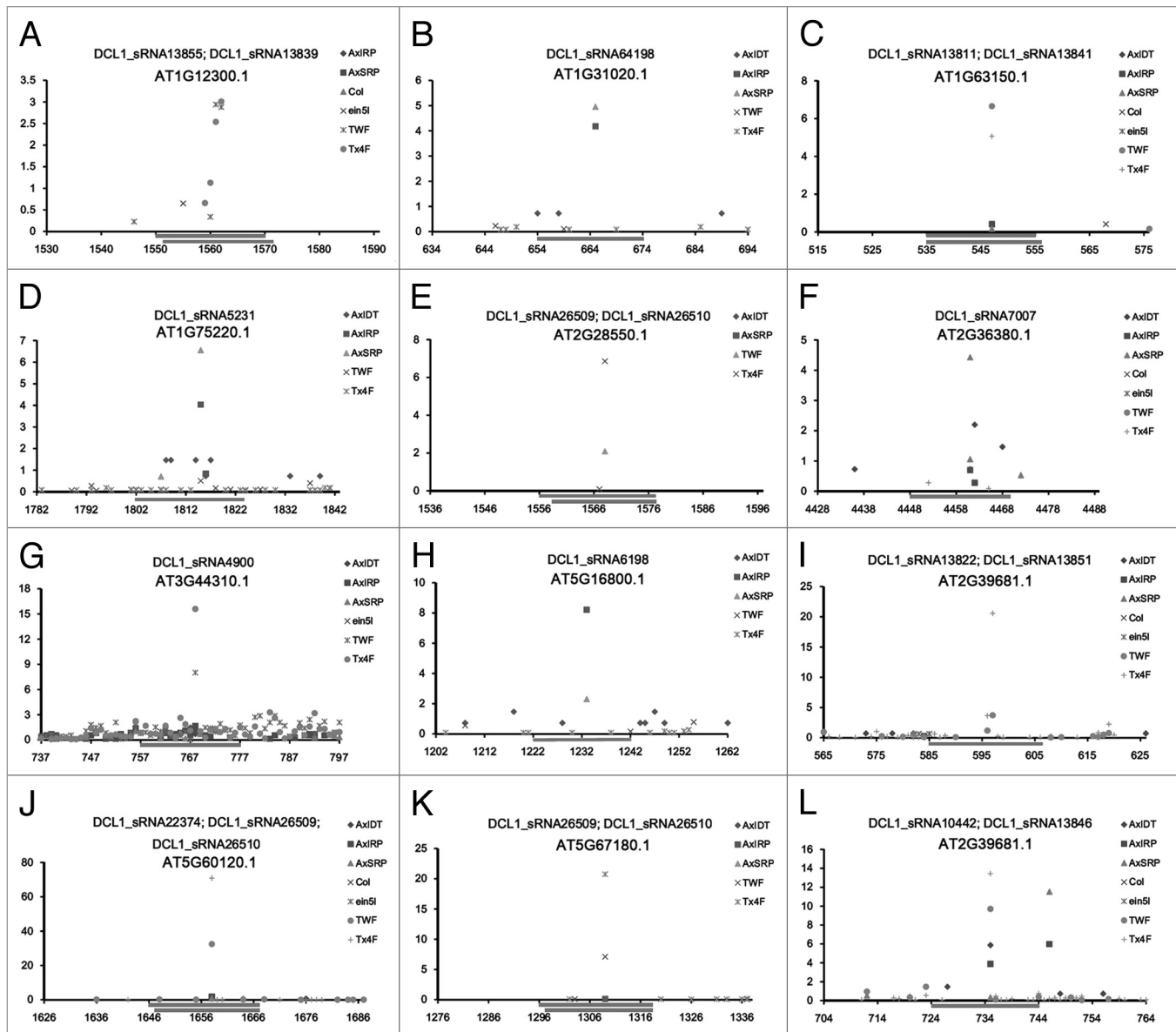


Figure 3. Degradome sequencing data-based identification of the transcripts targeted by the DCL1 (Dicer-like 1)-dependent, AGO1 (Argonaute 1)-enriched sRNAs (small RNAs) in *Arabidopsis*. Examples of identified targets are shown. For each figure panel, the target transcript ID and the corresponding sRNA(s) are listed on the top. The y axis measures the intensity (in RPM, reads per million) of the degradome signals, and the x axis indicates the position(s) of the cleavage signal(s) on the target transcript. The binding site of the sRNA regulator on its target transcript was denoted by a gray horizontal line. The figure keys for the signatures from different degradome sequencing libraries are shown on the right. Please note, for AT2G39681.1, two cleavage sites were identified.

Degradome and dsRNA sequencing data-based evidences supporting the origination of the DCL1-dependent sRNAs from the local long-stem structures of the lncRNAs

Although 65 006 of the 171,634 DCL1-dependent sRNAs could find their loci on the 5891 reported lncRNAs, whether lncRNAs are the genuine precursors for sRNA production through a DCL1-dependent way and how these sRNAs are generated remain unclear. To partially address the above issues, we set out to search for the cleavage signals produced during DCL1-mediated processing of the lncRNA precursors, and to search for the long-stem structures that could be potentially recognized by

DCL1 for dicing. It was based on the facts that: the stem region of a hairpin-structured miRNA precursor could be recognized by DCL1 for two-step processing,^{6,7} and the cropping sites of DCL1 on the miRNA precursors could be mapped by using degradome sequencing data in most cases.^{23,34}

The 154 106 loci of 65 006 DCL1-dependent sRNAs on the lncRNAs were included in this analysis. First, the publicly available degradome signatures were mapped onto the 5891 lncRNAs with sRNA loci. Then, we searched for the sRNA loci with degradome signatures mapped to either 5' or 3' ends which were considered to be the evidences for DCL1-mediated cropping

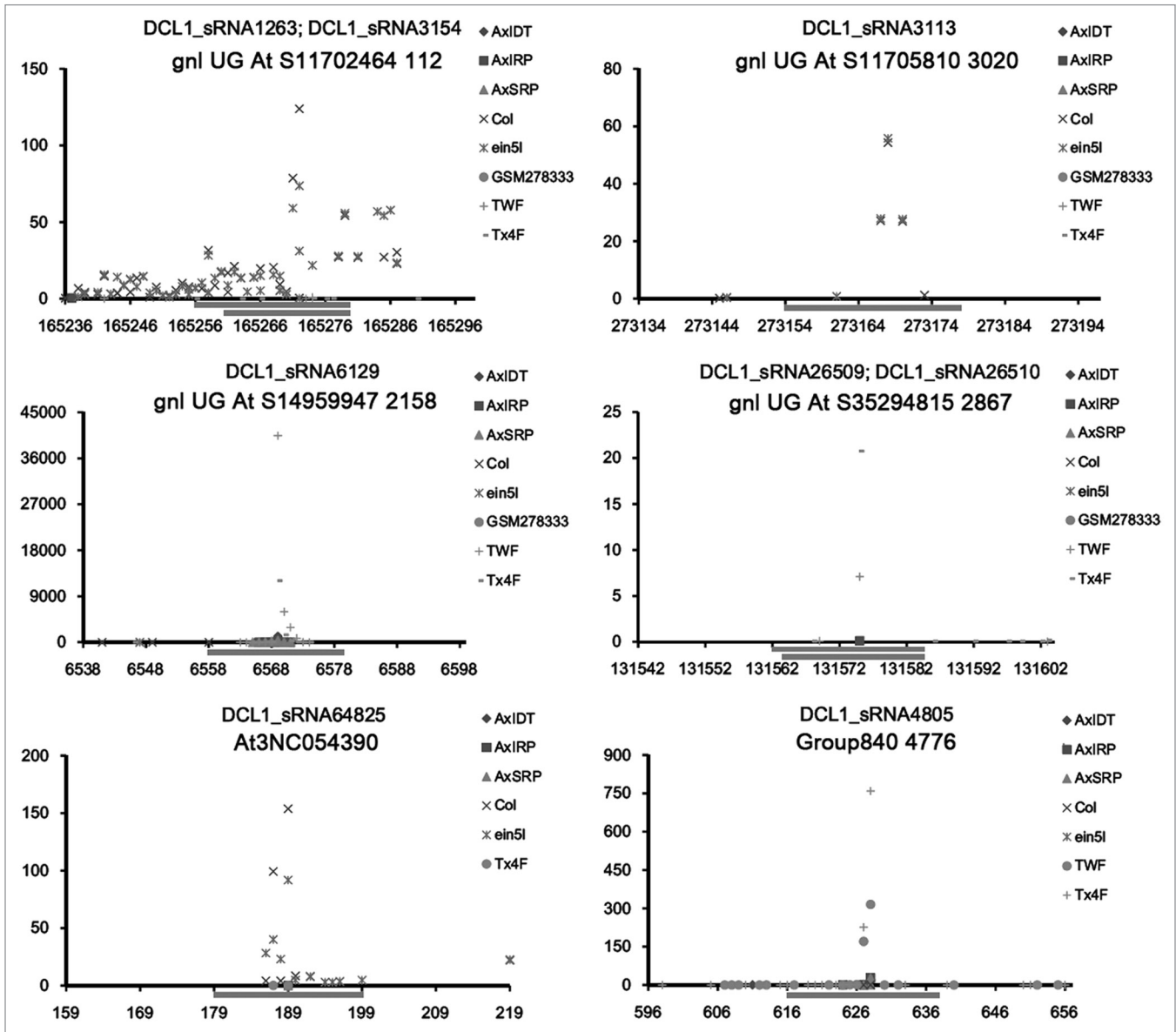


Figure 4. Degradome sequencing data-based identification of the lncRNAs (long non-coding RNAs) targeted by the DCL1 (Dicer-like 1)-dependent, AGO1 (Argonaute 1)-enriched sRNAs (small RNAs) in *Arabidopsis*. Examples of identified targets are shown. For each figure panel, the lncRNA ID and the corresponding sRNA(s) are listed on the top. The y axis measures the intensity (in RPM, reads per million) of the degradome signals, and the x axis indicates the position(s) of the cleavage signal(s) on the lncRNA. The binding site of the sRNA regulator on the lncRNA was denoted by a gray horizontal line. The figure keys for the signatures from different degradome sequencing libraries are shown on the right.

(Fig. 1B). As a result, 63 612 loci belonging to 19 012 sRNAs on 3084 lncRNAs were identified to be supported by degradome sequencing data. Strikingly, all of the supportive degradome signatures were found at the 5' ends of the sRNA loci, indicating the higher stability of the 5' cleaved remnants relative to the 3' cleaved ones.

The data generated by dsRNA-seq was quite useful for interrogating the in vivo structures of long transcripts. One dsRNA-seq data set (GSM575244; with two-round rRNA depletion) contributed by a previous study¹³ was recruited for the following structure-based analysis. First, all the dsRNA-seq reads were mapped onto the 3084 lncRNAs with degradome

data-supported sRNA loci. Second, a degradome-supported sRNA locus was retained if it resided within a dsRNA-seq read-covered region of 100 nt or longer. As a result, 6606 loci belonging to 3189 sRNAs were identified. After combining the loci sharing the same regions, a total of 609 dsRNA-seq read-covered regions on 367 lncRNAs were obtained (Fig. 1B; Data S5). All of the 609 sequences were subjected to secondary structure prediction by using RNashapes,³⁵ since they were likely to form internal long-stem structures. Based on manual screening, the dsRNA-seq read-covered regions with degradome-supported sRNA loci on the predicted long stems were retained. A total of 43 long-stem structures on 39 lncRNAs were identified

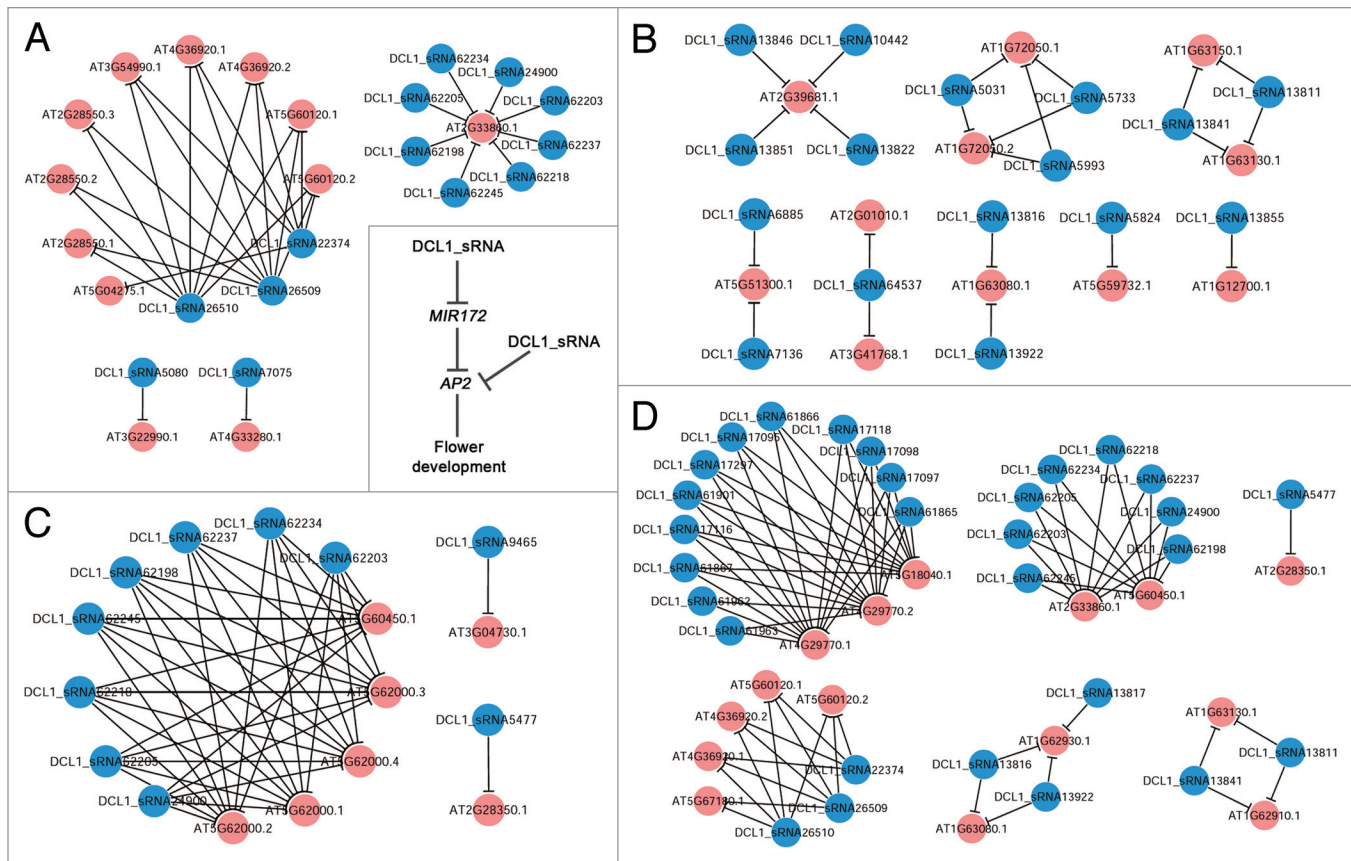


Figure 5. Biologically meaningful subnetworks identified from the target lists of the DCL1 (Dicer-like 1)-dependent, AGO1 (Argonaute 1)-enriched sRNAs (small RNAs) in *Arabidopsis*. (A) Subnetwork containing *AP2* (*APETALA2*)- and flower development-related target genes. (B) Subnetwork containing target genes involved in RNA-level biological processes such as processing, splicing and transcription. (C) Subnetwork containing target genes implicated in auxin signaling. (D) Subnetwork containing target genes whose expression levels were significantly upregulated in the *dcl1* mutant of *Arabidopsis* according to the previous reports.^{25,32,33} All the subnetworks were generated by using Cytoscape.⁴²

(Fig. S4). We observed that all of the 43 structures possess highly complementary long-stem regions encoding DCL1-dependent sRNAs (Fig. 6; Fig. S4), which strengthened the possibility of forming stabled internal structures within the lncRNAs. Taken together, based on degradome sequencing data, dsRNA-seq data and structure prediction, we provide further evidences to support the biogenesis model of the DCL1-dependent, lncRNA-originated sRNAs. We deduced that the 39 novel lncRNAs could serve as the sRNA precursors owing to their ability of forming the local long-stem structures (supported by secondary structure prediction and dsRNA-seq data) recognized by DCL1 for cropping (supported by degradome signatures). However, this notion still needs further experimental validations.

Conclusions

Our results indicate that 43 sequence regions on 39 lncRNAs could form local long-stem structures for sRNA production which relies on the activity of DCL1. The DCL1-dependent sRNAs with different sequence characteristics were associated with different AGO silencing complexes. Specifically, 96

DCL1-dependent, AGO1-enriched sRNAs possess great potential of performing target cleavages on 109 transcripts originated from 78 genes of *Arabidopsis*. Besides, 44 lncRNAs were discovered to be targeted by 23 DCL1-dependent, AGO1-enriched sRNAs. Summarily, our study could advance the current understanding on the biological roles of lncRNAs in plants.

Materials and Methods

Data sources

The sRNA HTS data sets used for the identification of DCL1-dependent sRNAs and AGO enrichment analysis were retrieved from GEO (Gene Expression Omnibus; <http://www.ncbi.nlm.nih.gov/geo/>).³⁶ The detailed information of these data sets has been shown in Figure 1A.

The mature miRNAs and the pre-miRNAs of *Arabidopsis* were obtained from miRBase (release 20; <http://www.mirbase.org/>).³⁷

The genomic information of lncRNAs (including five groups of lncRNAs, i.e., “lncRNA_EST analysis,” “lncRNA_tiling array analysis 1,” “lncRNA_tiling array analysis 2,” “lncRNA_RepTAS

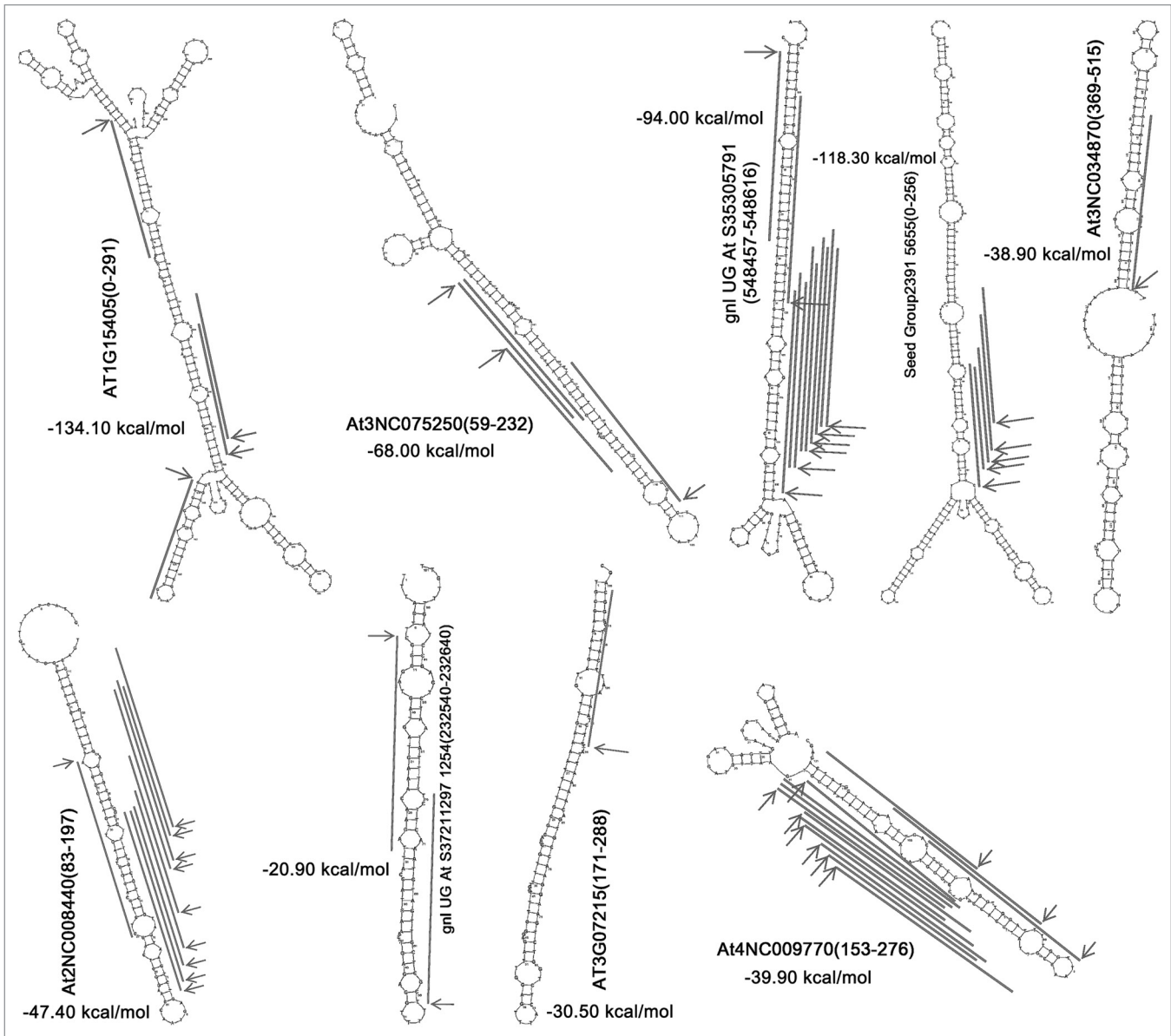


Figure 6. Examples of the DCL1 (Dicer-like 1)-dependent sRNA (small RNA) loci identified on the long-stem-structured regions of the lncRNAs (long non-coding RNAs) in *Arabidopsis*. For all the long-stem structures, the sequence ranges on the lncRNAs were shown in the brackets along with the lncRNA IDs. The DCL1-dependent sRNA loci were denoted by gray lines, and the degradome signature-based evidences for DCL1-mediated cleavages during sRNA generation were marked by gray arrows. All the secondary structures were predicted by using RNAshapes.³⁵ The minimum free energy (kcal/mol) of each optimal secondary structure was provided.

analysis” and “lncRNA_from TAIR”) was retrieved from PLncDB (<http://chualab.rockefeller.edu/gbrowse2/homepage.html>).¹² It was largely contributed by a previous study by Liu et al. (2012).¹¹ According to the above information, the lncRNA sequences were collected from the *Arabidopsis* Genome available in TAIR (The *Arabidopsis* Information Resource; release 9; <http://www.arabidopsis.org/>).³⁸

The dsRNA-seq data set GSM575244 (with two-round rRNA depletion; was retrieved from GEO) is a gift from a previous study by Zheng et al. (2010).¹³

The transcripts and the annotations of the genes were retrieved from TAIR (release 10; <http://www.arabidopsis.org/>).

The eight *Arabidopsis* degradome sequencing data sets (AxIDT, AxIRP, AxSRP, Col, ein5, TWF, Tx4F and GSM278333) were obtained from Next-Gen Sequence Databases (http://mpss.udel.edu/common/web/library_info.php?SITE=at_pare&showAll=true)³⁹ and GEO.

Prediction and validation of the sRNA targets

Target prediction was performed by using miRU algorithm^{19,20} with default parameters. The degradome sequencing data was utilized to validate the predicted sRNA—target pairs. First, in order to allow cross-library comparison, the normalized read count (in RPM, reads per million) of a short sequence from a specific degradome library was calculated by dividing the raw

count of this sequence by the total counts of the library, and then multiplied by 10^6 . Second, all the degradome signatures were mapped onto the predicted target transcripts. Then, the previously proposed criteria⁴⁰ were applied to extract the potential cleavage sites. Summarily, (1) “Average_Read count_Cleavage site” is the averaged read count (in RPM) of all the degradome signatures (belonging to one library) with their 5' ends mapped to a potential cleavage site; “Average_Read count_Surrounding” is the averaged read count of all the degradome signatures (also belonging to this library) that mapped to the regions surrounding the cleavage site; “Average_Read count_Cleavage site” should be five times or more than “Average_Read count_Surrounding.” (2) Also for this degradome library, among the degradome signatures mapped to a potential cleavage site, the most abundant tag should be among the top 12-most-abundant degradome signatures that perfectly mapped to the corresponding transcript. (3) The cleavage site should reside within 8–12 nt region of the regulatory sRNA. For any degradome library, if the three rules were fulfilled, the potential slicing sites were retained. Finally, both global and local target plots were drawn to perform manual screening, referring to our previous study.⁴¹ Only the transcripts with cleavage signals easy to be recognized were extracted as the potential sRNA—target pairs.

References

- Ozsolak F, Milos PM. RNA sequencing: advances, challenges and opportunities. *Nat Rev Genet* 2011; 12:87-98; PMID:21191423; <http://dx.doi.org/10.1038/nrg2934>
- Iaconetti C, Gareri C, Polimeni A, Indolfi C. Non-coding RNAs: the “dark matter” of cardiovascular pathophysiology. *Int J Mol Sci* 2013; 14:19987-20018; PMID:24113581; <http://dx.doi.org/10.3390/ijms141019987>
- Collins LJ, Penny D. The RNA infrastructure: dark matter of the eukaryotic cell? *Trends Genet* 2009; 25:120-8; PMID:19171405; <http://dx.doi.org/10.1016/j.tig.2008.12.003>
- Derrien T, Guigó R, Johnson R. The Long Non-Coding RNAs: A New (P)layer in the “Dark Matter”. *Front Genet* 2011; 2:107; PMID:22303401
- Bushati N, Cohen SM. microRNA functions. *Annu Rev Cell Dev Biol* 2007; 23:175-205; PMID:17506695; <http://dx.doi.org/10.1146/annurev.cellbio.23.090506.123406>
- Jones-Rhoades MW, Bartel DP, Bartel B. MicroRNAs and their regulatory roles in plants. *Annu Rev Plant Biol* 2006; 57:19-53; PMID:16669754; <http://dx.doi.org/10.1146/annurev.arplant.57.032905.105218>
- Voinnet O. Origin, biogenesis, and activity of plant microRNAs. *Cell* 2009; 136:669-87; PMID:19239888; <http://dx.doi.org/10.1016/j.cell.2009.01.046>
- De Lucia F, Dean C. Long non-coding RNAs and chromatin regulation. *Curr Opin Plant Biol* 2011; 14:168-73; PMID:21168359; <http://dx.doi.org/10.1016/j.pbi.2010.11.006>
- Wierzbicki AT. The role of long non-coding RNA in transcriptional gene silencing. *Curr Opin Plant Biol* 2012; 15:517-22; PMID:22960034; <http://dx.doi.org/10.1016/j.pbi.2012.08.008>
- Wu HJ, Wang ZM, Wang M, Wang XJ. Widespread long noncoding RNAs as endogenous target mimics for microRNAs in plants. *Plant Physiol* 2013; 161:1875-84; PMID:23429259; <http://dx.doi.org/10.1104/pp.113.215962>

Plant gene set enrichment analysis

The online tool PlantGSEA²⁵ was employed for this analysis. The IDs of all the target genes were submitted for enrichment analysis. “G1” (including “BP,” “CC” and “MF”), “G2,” “G3” (including “PlantCyc,” “KEGG,” “PO” and “Ref”) and “G4” (including “MIR” and “TFT”) were all selected for the analysis. *Arabidopsis thaliana* was chosen as the species analyzed, and “Suggested background (Whole genome level)” was chosen as the background.

Disclosure of Potential Conflicts of Interest

No potential conflicts of interest were disclosed.

Acknowledgments

We would like to thank all the publicly available data sets and the scientists behind them. This work was funded by the National Natural Science Foundation of China [31100937], [31125011] and [31271380], and the Starting Grant funded by Hangzhou Normal University to Yijun Meng [2011QDL60].

Supplemental Material

Supplemental Material may be found here: www.landesbioscience.com/journals/rnabiology/article/28725/

- Liu J, Jung C, Xu J, Wang H, Deng S, Bernad L, Arenas-Huertero C, Chua NH. Genome-wide analysis uncovers regulation of long intergenic noncoding RNAs in Arabidopsis. *Plant Cell* 2012; 24:4333-45; PMID:23136377; <http://dx.doi.org/10.1105/tpc.112.102855>
- Jin J, Liu J, Wang H, Wong L, Chua NH. PLncDB: plant long non-coding RNA database. *Bioinformatics* 2013; 29:1068-71; PMID:23476021; <http://dx.doi.org/10.1093/bioinformatics/btt107>
- Zheng Q, Ryvkin P, Li F, Dragomir I, Valladares O, Yang J, Cao K, Wang LS, Gregory BD. Genome-wide double-stranded RNA sequencing reveals the functional significance of base-paired RNAs in Arabidopsis. *PLoS Genet* 2010; 6:e1001141; PMID:20941385; <http://dx.doi.org/10.1371/journal.pgen.1001141>
- Wyman SK, Knouf EC, Parkin RK, Fritz BR, Lin DW, Dennis LM, Krouse MA, Webster PJ, Tewari M. Post-transcriptional generation of miRNA variants by multiple nucleotidyl transferases contributes to miRNA transcriptome complexity. *Genome Res* 2011; 21:1450-61; PMID:21813625; <http://dx.doi.org/10.1101/gr.118059.110>
- Lu S, Sun YH, Chiang VL. Adenylation of plant miRNAs. *Nucleic Acids Res* 2009; 37:1878-85; PMID:19188256; <http://dx.doi.org/10.1093/nar/gkp031>
- Chen X. Small RNAs and their roles in plant development. *Annu Rev Cell Dev Biol* 2009; 25:21-44; PMID:19575669; <http://dx.doi.org/10.1146/annurev.cellbio.042308.113417>
- Vaucheret H. Plant ARGONAUTES. *Trends Plant Sci* 2008; 13:350-8; PMID:18508405; <http://dx.doi.org/10.1016/j.tplants.2008.04.007>
- Mi S, Cai T, Hu Y, Chen Y, Hodges E, Ni F, Wu L, Li S, Zhou H, Long C, et al. Sorting of small RNAs into Arabidopsis argonaute complexes is directed by the 5' terminal nucleotide. *Cell* 2008; 133:116-27; PMID:18342361; <http://dx.doi.org/10.1016/j.cell.2008.02.034>
- Dai X, Zhao PX. psRNATarget: a plant small RNA target analysis server. *Nucleic Acids Res* 2011; 39:W155-9; PMID:21622958; <http://dx.doi.org/10.1093/nar/gkr319>
- Zhang Y. miRU: an automated plant miRNA target prediction server. *Nucleic Acids Res* 2005; 33:W701-4; PMID:15980567; <http://dx.doi.org/10.1093/nar/gki383>
- Addo-Quaye C, Eshoo TW, Bartel DP, Axtell MJ. Endogenous siRNA and miRNA targets identified by sequencing of the Arabidopsis degradome. *Curr Biol* 2008; 18:758-62; PMID:18472421; <http://dx.doi.org/10.1016/j.cub.2008.04.042>
- Addo-Quaye C, Snyder JA, Park YB, Li YF, Sunkar R, Axtell MJ. Sliced microRNA targets and precise loop-first processing of MIR319 hairpins revealed by analysis of the Physcomitrella patens degradome. *RNA* 2009; 15:2112-21; PMID:19850910; <http://dx.doi.org/10.1261/rna.1774909>
- Li YF, Zheng Y, Addo-Quaye C, Zhang L, Saini A, Jagadeeswaran G, Axtell MJ, Zhang W, Sunkar R. Transcriptome-wide identification of microRNA targets in rice. *Plant J* 2010; 62:742-59; PMID:20202174; <http://dx.doi.org/10.1111/j.1365-3113X.2010.04187.x>
- Llave C, Xie Z, Kasschau KD, Carrington JC. Cleavage of Scarecrow-like mRNA targets directed by a class of Arabidopsis miRNA. *Science* 2002; 297:2053-6; PMID:12242443; <http://dx.doi.org/10.1126/science.1076311>
- Yi X, Du Z, Su Z. PlantGSEA: a gene set enrichment analysis toolkit for plant community. *Nucleic Acids Res* 2013; 41:W98-103; PMID:23632162; <http://dx.doi.org/10.1093/nar/gkt281>
- Jofuku KD, den Boer BG, Van Montagu M, Okamoto JK. Control of Arabidopsis flower and seed development by the homeotic gene APETALA2. *Plant Cell* 1994; 6:1211-25; PMID:7919989
- Okamoto JK, Szeto W, Lotys-Prass C, Jofuku KD. Photo and hormonal control of meristem identity in the Arabidopsis flower mutants apetala2 and apetala1. *Plant Cell* 1997; 9:37-47; PMID:9014363
- Bowman JL, Smyth DR, Meyerowitz EM. Genes directing flower development in Arabidopsis. *Plant Cell* 1989; 1:37-52; PMID:2535466

29. Aukerman MJ, Sakai H. Regulation of flowering time and floral organ identity by a MicroRNA and its APETALA2-like target genes. *Plant Cell* 2003; 15:2730-41; PMID:14555699; <http://dx.doi.org/10.1105/tpc.016238>
30. Chen X. A microRNA as a translational repressor of APETALA2 in Arabidopsis flower development. *Science* 2004; 303:2022-5; PMID:12893888; <http://dx.doi.org/10.1126/science.1088060>
31. Wang JW, Wang LJ, Mao YB, Cai WJ, Xue HW, Chen XY. Control of root cap formation by MicroRNA-targeted auxin response factors in Arabidopsis. *Plant Cell* 2005; 17:2204-16; PMID:16006581; <http://dx.doi.org/10.1105/tpc.105.033076>
32. Nodine MD, Bartel DP. MicroRNAs prevent precocious gene expression and enable pattern formation during plant embryogenesis. *Genes Dev* 2010; 24:2678-92; PMID:21123653; <http://dx.doi.org/10.1101/gad.1986710>
33. Xie Z, Allen E, Wilken A, Carrington JC. DICER-LIKE 4 functions in trans-acting small interfering RNA biogenesis and vegetative phase change in Arabidopsis thaliana. *Proc Natl Acad Sci U S A* 2005; 102:12984-9; PMID:16129836; <http://dx.doi.org/10.1073/pnas.0506426102>
34. Meng Y, Gou L, Chen D, Wu P, Chen M. High-throughput degradome sequencing can be used to gain insights into microRNA precursor metabolism. *J Exp Bot* 2010; 61:3833-7; PMID:20643809; <http://dx.doi.org/10.1093/jxb/erq209>
35. Steffen P, Voss B, Rehmsmeier M, Reeder J, Giegerich R. RNAshapes: an integrated RNA analysis package based on abstract shapes. *Bioinformatics* 2006; 22:500-3; PMID:16357029; <http://dx.doi.org/10.1093/bioinformatics/btk010>
36. Barrett T, Troup DB, Wilhite SE, Ledoux P, Rudnev D, Evangelista C, Kim IF, Soboleva A, Tomashevsky M, Marshall KA, et al. NCBI GEO: archive for high-throughput functional genomic data. *Nucleic Acids Res* 2009; 37:D885-90; PMID:18940857; <http://dx.doi.org/10.1093/nar/gkn764>
37. Griffiths-Jones S, Saini HK, van Dongen S, Enright AJ. miRBase: tools for microRNA genomics. *Nucleic Acids Res* 2008; 36:D154-8; PMID:17991681; <http://dx.doi.org/10.1093/nar/gkm952>
38. Huala E, Dickerman AW, Garcia-Hernandez M, Weems D, Reiser L, LaFond F, Hanley D, Kiphart D, Zhuang M, Huang W, et al. The Arabidopsis Information Resource (TAIR): a comprehensive database and web-based information retrieval, analysis, and visualization system for a model plant. *Nucleic Acids Res* 2001; 29:102-5; PMID:11125061; <http://dx.doi.org/10.1093/nar/29.1.102>
39. Nakano M, Nobuta K, Vemaraju K, Tej SS, Skogen JW, Meyers BC. Plant MPSS databases: signature-based transcriptional resources for analyses of mRNA and small RNA. *Nucleic Acids Res* 2006; 34:D731-5; PMID:16381968; <http://dx.doi.org/10.1093/nar/gkj077>
40. Shao C, Chen M, Meng Y. A reversed framework for the identification of microRNA-target pairs in plants. *Brief Bioinform* 2013; 14:293-301; PMID:22811545; <http://dx.doi.org/10.1093/bib/bbs040>
41. Meng Y, Shao C, Chen M. Toward microRNA-mediated gene regulatory networks in plants. *Brief Bioinform* 2011; 12:645-59; PMID:21262742; <http://dx.doi.org/10.1093/bib/bbq091>
42. Shannon P, Markiel A, Ozier O, Baliga NS, Wang JT, Ramage D, Amin N, Schwikowski B, Ideker T. Cytoscape: a software environment for integrated models of biomolecular interaction networks. *Genome Res* 2003; 13:2498-504; PMID:14597658; <http://dx.doi.org/10.1101/gr.1239303>